In situ determination of photobioproduction of H_2 by In_2S_3-[NiFeSe] Hydrogenase from *Desulfovibrio vulgaris Hildenborough* using only visible light.

Journal:	*ACS Catalysis*
Manuscript ID	cs-2016-01512p
Manuscript Type:	Article
Date Submitted by the Author:	30-May-2016
Complete List of Authors:	Pita, Marcos; ICP-CSIC, Biocatalysis De Lacey, Antonio; CSIC, Instituto de Catalisis Conesa, José; Consejo Superior de Investigaciones Científicas, Instituto de Catálisis y Petroleoquímica Pereira, Inês; ITQB-UNL, Microbial Biochemistry Zacarias, Sonia; ITQB-UNL, Microbial Biochemistry Tapia, Cristina; ICP-CSIC, Biocatalysis

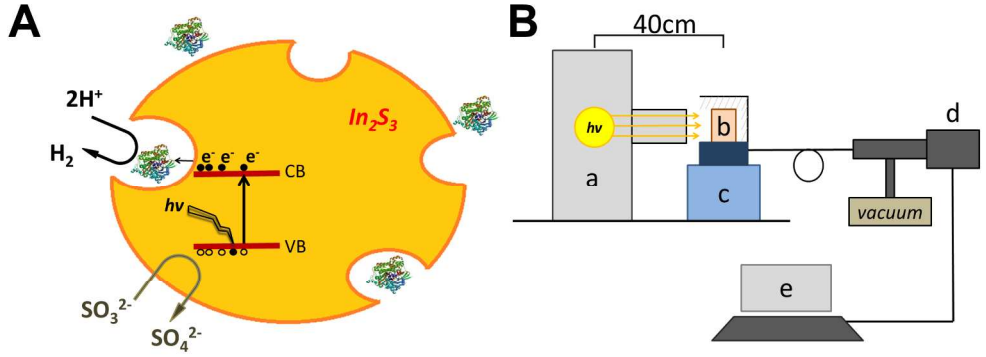

Scheme 1. A) In2S3/Hase hybrid for photocatalytic production of H2 using sulfite as sacrificial compound. B) Experimental setup for measuring H2 photoproduction: a) xenon lamp, b) reactor, c) magnetic stirrer, d) mass spectrometer, e) computer.
237x91mm (300 x 300 DPI)

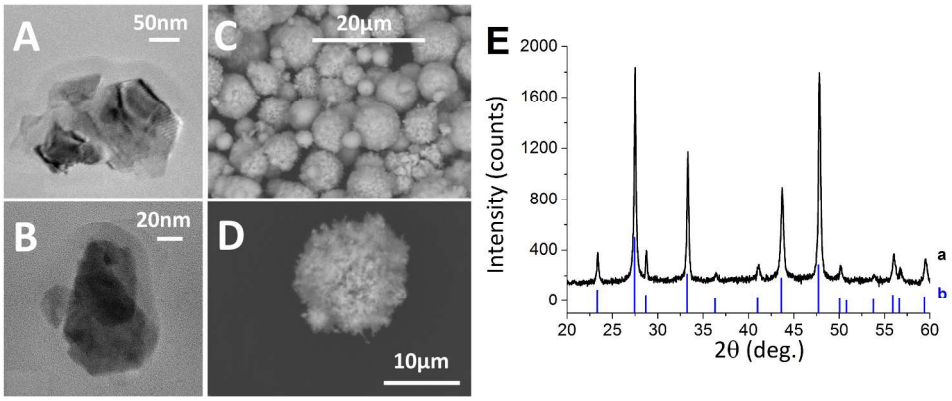

Figure 1. (A, B) TEM images showing two different particles of In2S3. (C, D) SEM images from panoramic and magnified In2S3 powder aggregates, respectively. (E) (a) XRD Diffractogram obtained from the synthesized In2S3. (b) XRD reference pattern of In2S3 (ref. code 01- 084-1385)
440x173mm (300 x 300 DPI)

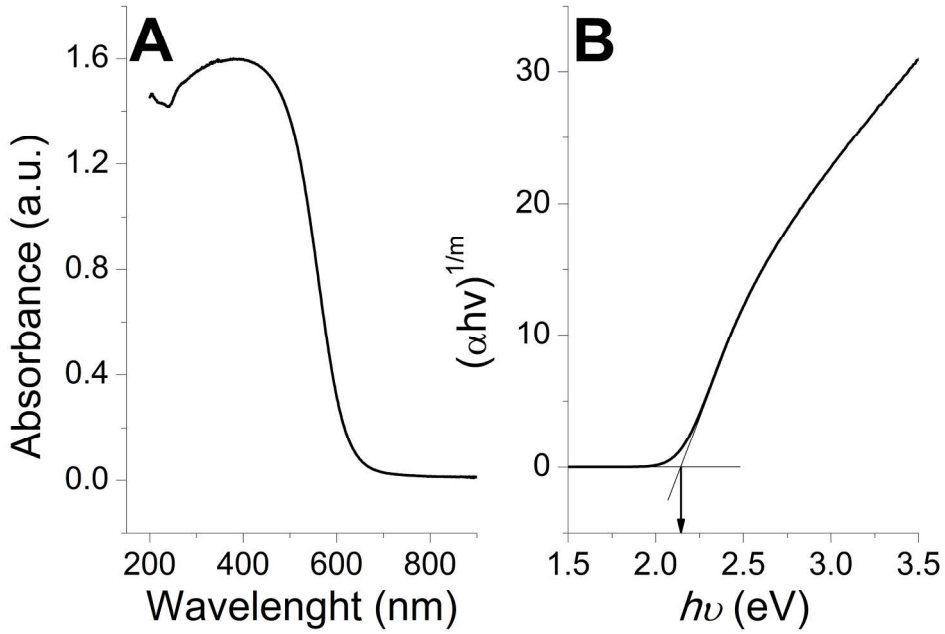

Figure 2. A) UV/Vis absorbance spectrum of In2S3. B) Plot of direct band gap of In2S3, where α corresponds to absorption coefficient, h corresponds to Plank Constant, υ to incident photon frequency and m correspond to the transition (m=1/2 for direct transition). The arrow marks the band gap value of the semiconductor.
192x135mm (300 x 300 DPI)

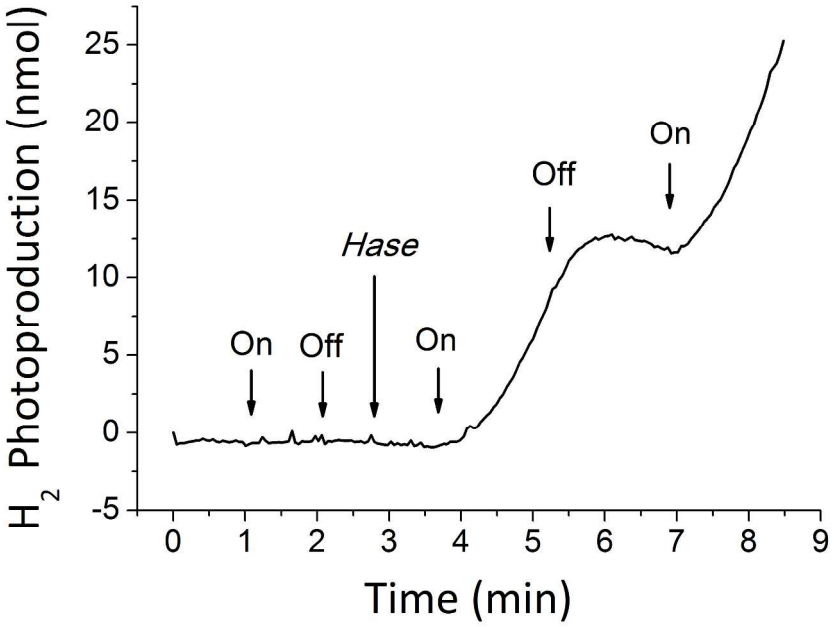

Figure 3. Photocatalytic production of H2 by Dv. [NiFeSe] Hase mixed with In2S3 particles monitored by mass spectrometry. The measurements were performed at 37°C in 50mM Tris-HCl, 0.2 M sodium sulfite at pH 7. The arrows mark the times at which the lamp was turned on or off and of Hase injection into the reactor vessel.
274x192mm (300 x 300 DPI)

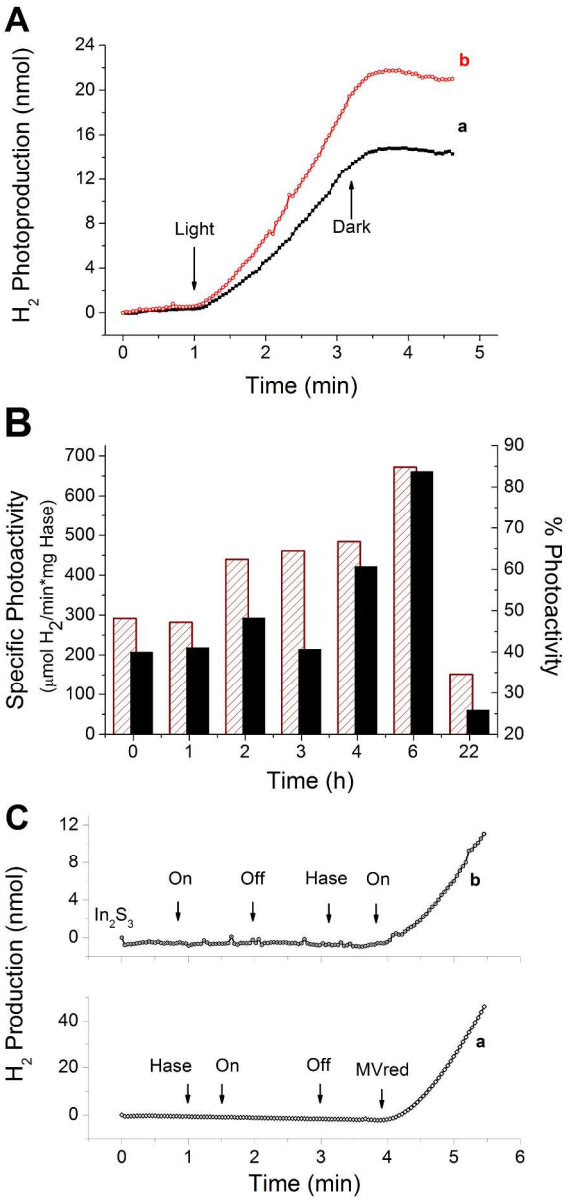

Figure 4. Photocatalytic production of H2 by Dv. [NiFeSe] Hase in combination with In2S3 particles monitored by mass spectrometry. Measurements were performed at 37°C in 50 mM Tris-HCl 0.2 M sodium sulfite at pH 7. (A) The lines represent H2 evolution with no previous incubation of the enzyme with the In2S3 (a) or after 3 hours of incubation of Hase with In2S3 at 4°C in a roller mixer (b). (B) Striped column bars represent the specific activity of H2 photoproduction by Hase after different incubation times. Black column bars represent the % of photoactivity of Hase compared to the specific activity of the sample measured with reduced MV as electron donor. (C) Negative controls of photoactivity monitored by mass spectrometry. The lines represent the H2 evolution under white light illumination with only Hase (a) and only In2S3 (b). The arrows mark the time when the light is on or off and the moment when 10µL of 0.166µM Hase or 2 µL of 1 M sodium dithionite is injected into the vessel to reduce the MV.
160x334mm (300 x 300 DPI)

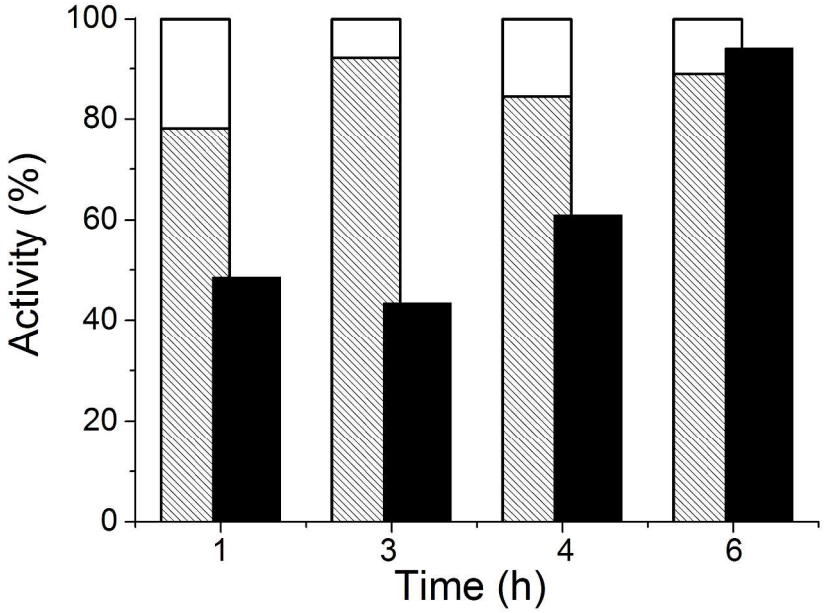

Figure 5. Percentage of Dv. [NiFeSe] Hase activity retained by In2S3 particles after incubation periods of 1, 3, 4 and 6 hours. The white and striped bar areas represent the % of Hase activity (measured with reduced MV) in the supernatant and In2S3 particles fractions respectively. Black bars represent the % of H2 photobiocatalytic production in the In2S3 particles fraction compared to the Hase activity with reduced MV. Measurements were done at 37°C in 50 mM Tris-HCl 0.2 M sodium sulfite at pH 7.
274x192mm (300 x 300 DPI)

In situ determination of photobioproduction of H_2 by In_2S_3-[NiFeSe] Hydrogenase from *Desulfovibrio vulgaris* Hildenborough using only visible light.

Cristina Tapia[a], Sonia Zacarias[b], Inês A. C. Pereira[b], Jose C. Conesa[a], Marcos Pita[a], Antonio L. De Lacey*[a]*

[a] Instituto de Catálisis y Petroleoquímica, CSIC. c/ Marie Curie 2, 28049 Madrid (Spain).

[b] Instituto de Tecnologia Quimica e Biologica. Universidade Nova de Lisboa. Apartado 127, 2781-901 Oeiras (Portugal).

KEYWORDS: Hydrogenase, In_2S_3, Biocatalysis, Photocatalysis, Visible light, Hydrogen.

ABSTRACT. An interesting strategy for photocatalytic production of hydrogen from water and sunlight is the formation of a hybrid photocatalyst that combines an inorganic semiconductor able to absorb in the visible light spectral range with an enzymatic catalyst for reducing protons. In this work we study how to optimize the interfacing of In_2S_3 particles with the soluble form of [NiFeSe] hydrogenase from *Desulfovibrio vulgaris* Hildenborough by means of its initial H_2 photoproduction rate. The kinetics of the photocatalytic process was studied by membrane-inlet

mass spectrometry, in order to optimize the interaction between both components of the hybrid photocatalyst. Membrane-inlet mass spectrometry allows measuring in the same experiment, for comparison, the rate of H_2 production by the photocatalyst hybrid directly in the aqueous solution in real time and the result of a standard assay of the hydrogenase activity. An incubation period of 6 hours under mild stirring of hydrogenase with In_2S_3 particles was necessary for optimal interaction of the enzyme molecules with the porous surface of the semiconductor. A turnover frequency of the NiFeSe Hydrogenase (TOF_{Hase}) for H_2-photobioproduction of 986 s^{-1} was measured under the optimized conditions. This means that the immobilized hydrogenase has a photocatalytic efficiency for H_2 generation which is 94% of that obtained in the standard specific activity test of H_2 production using reduced methyl viologen as electron donor.

Introduction

Hydrogen is considered a clean energy vector, although nowadays most hydrogen is still produced from fossil fuels or by water electrolysis using noble metals as electrocatalysts.[1] Therefore, efficient photocatalytic production of hydrogen from water and sunlight is currently a major goal of research towards a sustainable energy generation.[2] An interesting strategy for this purpose is the formation of a hybrid photocatatalyst that combines an inorganic semiconductor able to absorb in the visible light spectral range with a non-noble metal inorganic[3] or enzymatic[4] catalyst for reducing protons. Many metal sulfide semiconductors have attracted much attention due to their band gap in the energy range of visible light radiation and their conduction band energy level situated above that required for reducing protons.[5] Some of them, specially CdS, have shown excellent properties for photocatalytic production of hydrogen under visible light in

aqueous solution using a co-catalyst and a sacrificial compound for holes replenishment.[6] In_2S_3 is another semiconductor frequently used as buffer layer in photovoltaic solar cells[7] or water splitting photochemical cells[8] because of its interesting electron handling properties. It has also other potential applications such as visible-light driven photodegradation of organic dyes.[9] In_2S_3 is also of interest in photocatalytic production of hydrogen due to its similar band gap energy (Eg≈2-2.3eV) to that of CdS, conduction band potential of -0.8V *vs* RHE and lower toxicity.[5] In_2S_3 is easily synthesized by solvothermal reaction with no further modification being needed.[10]

In the present work we study a hybrid system based on In_2S_3 semiconductor and an enzymatic co-catalyst for proton reduction in aqueous solution. Hydrogenases are redox metalloproteins that catalyze efficiently H_2 production and oxidation under mild conditions.[11] Hydrogenases are classified according to their metal content of their redox centers. The main groups of hydrogenases are the [NiFe] and the [FeFe] Hydrogenases, which have a bimetallic complex coordinated by thiolates, CO and CN^- ligands as catalytic site for H_2 oxidation/production, and have an electron transfer pathway formed by iron-sulfur clusters that connect the active site with the enzyme surface.[12] Hydrogenases have shown an excellent electrocatalytic activity with a turnover frequency (TOF) up to 10,000 s^{-1} when attached to electrodes.[13] Hydrogenases have also shown to be good catalysts for photocatalytic hydrogen production when adsorbed on TiO_2,[14] CdS[15], CdTe[16] or carbon nitride[17] semiconductors. In particular, [NiFeSe] hydrogenases are well suited for this purpose because they have a high H_2 production activity, operational stability and tolerance to oxygen under reducing conditions.[14,17,18] [NiFeSe] hydrogenases are a subgroup of the [NiFe] hydrogenases that contain a selenocysteine instead of a cysteine as one of the ligands to the nickel of its active site, which has a redox potential of around -0.400V (*vs* NHE).[19]

A critical step for the rate of photocatalytic hydrogen production is the electron transfer between the conduction band of the semiconductor and the co-catalyst, in order to minimize charge recombination in the semiconductor.[3a,20] This issue is especially evident in the case of using hydrogenases as co-catalysts, in which interfacial electron transfer at the semiconductor surface is the rate-limiting step of the photocatalytic process.[17,21] Therefore, efforts are needed to optimize this interaction between the enzyme molecules and the semiconductor particles, so that the overall rates of photocatalytic H_2 production reach values near to the high turnover rates of hydrogenases. The Hase-In_2S_3 electron transfer will be here studied in terms of initial rates of H_2 production, which is the regime where more reliable data are produced.

This work will show the very first study on the production of hydrogen with a hybrid photocatalyst composed by In_2S_3 particles and the soluble form of [NiFeSe] hydrogenase from *Desulfovibrio vulgaris* Hildenborough. In_2S_3 has been chosen because it works under visible light rather than UV like TiO_2[14], whereas being Cd-free makes it less toxic than CdS[15] and CdTe[16]. In order to optimize the interaction between both components of the hybrid photocatalyst we studied the kinetics of the photocatalytic process by membrane-inlet mass spectrometry. In this method the reactor for the photocatalytic process has no gas phase and is connected through a Teflon membrane to the high vacuum line of a mass spectrometer (Scheme 1).[22] This setup allows to measure the rate of H_2 production directly in the aqueous solution in real time, which gives us valuable information of the interface process occurring between the hydrogenase and semiconductor.

Scheme 1. A) In_2S_3/Hase hybrid for photocatalytic production of H_2 using sulfite as sacrificial compound. B) Experimental setup for measuring H_2 photoproduction: a) xenon lamp, b) reactor, c) magnetic stirrer, d) mass spectrometer, e) computer.

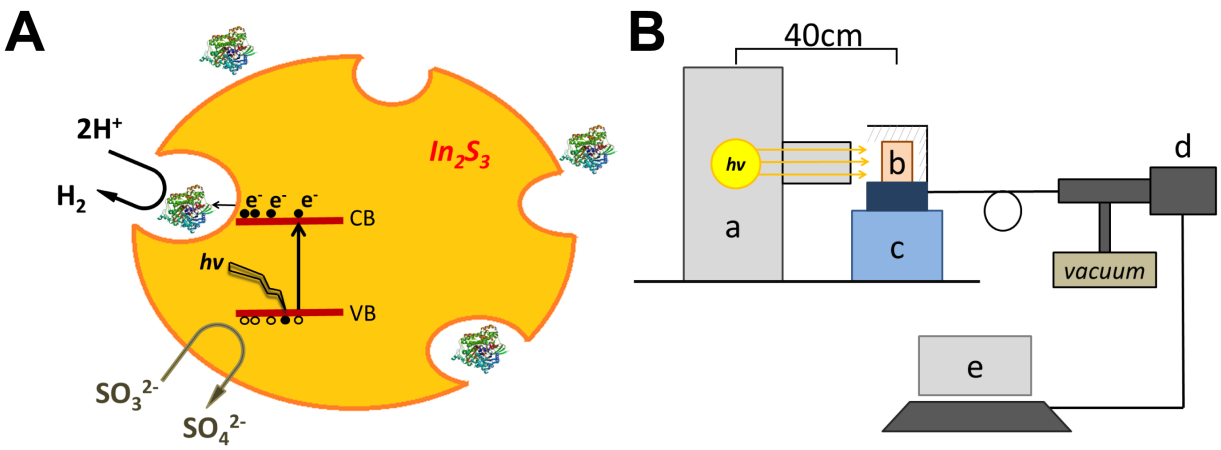

Material and Methods

Reagents.

All the reagents were used as received without further purification. $InCl_3$ 99.999%, thiourea 99%, sodium sulfite 98%, TRIS (hydroxymethyl)-aminomethane 99%, HEPES 99.5% and methyl viologen dichloride 98% (MV) were purchased from Sigma-Aldrich. Sodium acetate 99.5% was purchased from Fluka. Sodium hydrogen carbonate 99.999% and hydrochloric acid 37% were purchased from Panreac. Sodium dithionite 87% was purchased from MERK and absolute ethanol was purchased from Scharlau. Low density graphite (LDG, 99.999% purity) rods of 3.05 mm diameter were obtained from Alfa Aesar. Aqueous solutions were prepared using MilliQ deionized water (18.2 MΩ × cm). H_2 99.999%, 20% H_2: 80% Ar and Ar 99.999% bottles were supplied by Air Liquide.

Synthesis of In_2S_3.

The polycrystalline powder of In_2S_3 was synthetized following a known hydrothermal procedure.[10] A Teflon-lined steel high-pressure reactor containing a Pyrex beaker was filled with 50 mL of aqueous solution containing 148 mM $InCl_3$ and 178 mM thiourea. 80 μL of HCl 37% were added to acidify the solution and the reactor was set into a stove at 435 K during 48 hours.

The reaction product was centrifuged during 15 min at 20°C and 7000 rpm using a BECKMAN Coulter Avanti J-E centrifuge with a JA 25.5 rotor. The supernatant was discarded and the solid was redispersed in distilled water. This process was repeated twice. Finally, another centrifugation-redispersion cycle was carried out using EtOH. The resulting solid was set to dry for 12 hours at 60°C (Figure S1 of Supporting Information). The reaction yield was 80%.

Characterization techniques.

X-Ray Diffraction (XRD) of the synthesized In_2S_3 powder was performed with a Philips X'Pert Pro PANalytical diffractometer (Cu-Kα, λ= 0.1541874 nm).

Scanning electron microscopy (SEM) was performed with a TM-1000 Tabletop Hitachi including an X-ray Dispersive Energy detector (EDX).

Transmission electron microscopy (TEM) was performed at a point resolution of 0.19 nm with a 200KV JEOL 2100 transmission electron microscope, equipped with an Oxford Instruments EDX analyzer. Samples were prepared by taking the powder into an ethanol-filled Eppendorf and immersed during 15 min into an ultrasound bath. 20 μL of the sample were deposited on a carbon film-coated 200 mesh copper TEM grid (Electron Microscopy Sciences) and let to dry.

The UV-Vis spectrum of the powder was measured using a double beam UV-Vis-NIR Varian Cary 5000 spectrometer.

The surface area of In_2S_3 particles was measured using the Brunauer-Emmett-Teller (BET) method calculation with an Isotherms of Absorption ASAP2020 Micromeritics equipment, after 100 h of N_2 degassification at room temperature.

Voltamperometry and impedance measurements were recorded with an Autolab Potentiostat/Galvanostat Ecochemie PGSTAT30 with a Frequency Response Analysis (FRA) module. Impedance measurements were performed at 1000 Hz and 0.482 V vs. NHE. A three-

electrode cell configuration was used with an aqueous electrolyte containing 0.1 M sodium carbonate, 0.1 M sodium acetate and 0.1 M sodium sulfite in the pH range of 4-10. The working electrode was prepared by depositing 6 μL of a 30 mg In_2S_3 suspension in 1 mL of EtOH onto a clean LDG rod, and dried at 100°C under vacuum during 2 hours. The reference electrode was Ag/AgCl (3 M NaCl) from BAS and a Pt wire (0.5 mm diameter, Goodfellow) was used as counter electrode. Cyclic voltammetry for the electrochemical characterization of In_2S_3 was performed using a LDG-In_2S_3 working electrode in 100 mM phosphate buffer pH 7.5.

D. vulgaris [NiFeSe] hydrogenase purification and catalytic activity assay.

The recombinant soluble form of *D. vulgaris* Hildenborough [NiFeSe] hydrogenase (Hase) was isolated and purified with a molecular weight of 85 kDa as reported.[23] The H_2-production activity of the enzyme was measured by membrane-inlet mass spectrometry.[24] The output signal of the mass spectrometer (Pfeiffer Prisma) for each mass value expressed as a current signal is proportional to the concentration of H_2 dissolved in the reaction vessel.[24] The output signal of the spectrometer for mass 2 was calibrated first by saturating the reactor solution with 100% H_2. The catalytic activity of the hydrogenase was measured in a 10 mL solution of 1 mM MV in pH 7.0, 50 mM Tris-HCl buffer. The solution was purged with 100% Ar and then the reactor was closed, leaving no gas phase inside. A 10μL solution of 0.166 μM Hase, previously activated under H_2 atmosphere as said below, was injected to the reactor through a rubber septum with gastight syringes (SGE Analytical Science). The mass spectrometer was set to monitor mass 2 (H_2 production) and the reaction was initiated by injecting 2 μL of 1 M sodium dithionite into the vessel for reducing the methyl viologen. The Hase activation process consisted on adding 1 μL of 10 mM sodium dithionite to 50 μL of anaerobic enzyme solution in a glass vial with a rubber

Suba Seal septum (Sigma-Aldrich) and then incubating the solution under 100% H_2 atmosphere during 10 min at room temperature.

Photocatalytic hydrogen production by the D. vulgaris [NiFeSe]Hase-In_2S_3 hybrid.

A typical experiment was started by incubating at 4°C 0.26 pmol of Hase with 22.1 μmol of In_2S_3 in 10 mL of 50 mM Tris-HCl, pH 7.0 solution containing 0.2 M sodium sulfite. Sulfite was selected as electron donor according to published work.[6a] Alternative sacrificial electron donors such as acetate or sodium sulfide were tested in the preliminary study of the system, finding out that they were not as effective (data not shown). The suspension was stirred at 60 rpm speed on a roller mixer (SRT9D). The incubation times monitored were 1, 2, 3, 4, 6 and 22 hours. Each aliquot of In_2S_3-Hase mixture was placed in the reactor vessel connected to the mass spectrometer, which was closed avoiding the presence of a gas phase for measuring the photoproduction of H_2. The Hase was activated by bubbling the solution with 20% H_2: 80% Ar gas mixture during 10 minutes. Afterwards 100% Ar was bubbled to remove all the H_2 from the solution (monitorised by the decrease of mass 2 signal). Finally, the reactor was irradiated with white light coming from a Solar simulator 450W Xenon lamp. The distance from the light source to the reactor was 40 cm (Scheme 1). A black box covered the experimental setup to avoid any light reaching the reaction vessel except that produced by the xenon lamp. The power of light source was measured with a Delta OHM HD 2302.0 LightMeter, yielding 1.5 ± 0.1 W x m^{-2} within the range 315 – 400 nm and 368 ± 1 W x m^{-2} within the range 400 – 1050 nm. The rate of H_2 photoproduction in the reactor solution was measured by monitoring the evolution of mass 2 signal with time at the mass spectrometer. Control experiments were performed in absence either of semiconductor or hydrogenase under equal setup conditions.

Results

Semiconductor Characterization

The In_2S_3 powder obtained by the hydrothermal synthetic route described above displayed an orange-reddish colour (Fig. S1) and was characterized by different techniques. Transmission and Scanning electron microscopies (TEM-SEM) were used to determine the geometry and size of the powder particles.

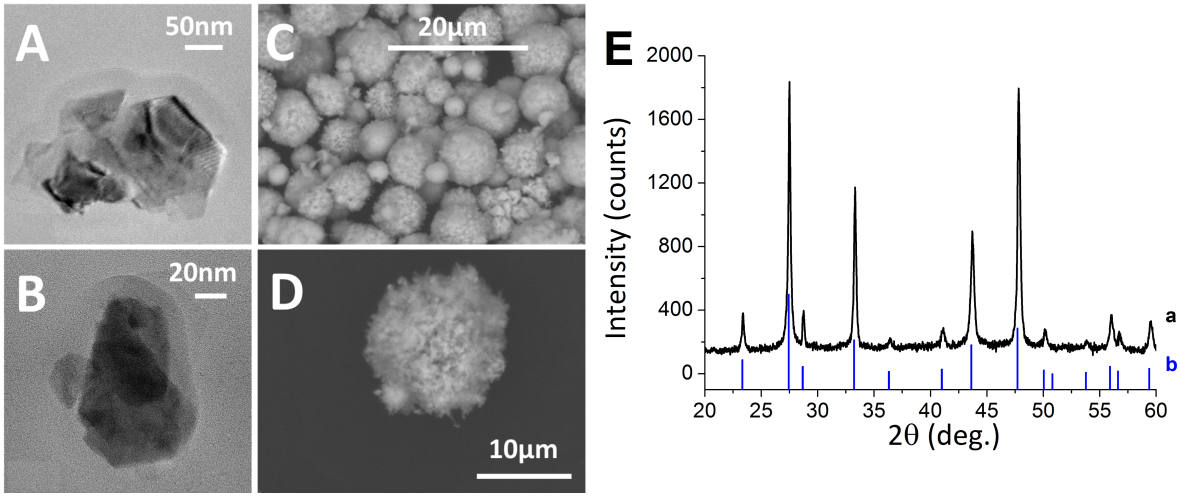

Figure 1. (A, B) TEM images showing two different particles of In_2S_3. (C, D) SEM images from panoramic and magnified In_2S_3 powder aggregates, respectively. (E) (a) XRD Diffractogram obtained from the synthesized In_2S_3. (b) XRD reference pattern of In_2S_3 (ref. code 01- 084-1385)

The TEM images show two typical In_2S_3 particles ranging 50-100 nm in diameter, with near-hexagonal shape (Figure 1A,B). It can also be appreciated that the particles comprise several crystalline domains, separated by typical grain boundaries. Scanning electron microscope revealed spherical particle aggregation with a broad distribution of sizes, which range from 2 to 15 μm of diameter (Figure 1C,D). The XRD diffractogram is displayed in Figure 1E, where (a) is the experimental XRD from the powder and (b) is the reference diffractogram, indicating the Miller indices, of cubic α-In_2S_3. The latter is a spinel structure with disordered cation vacancies,

usually obtained in this type of preparations instead of the thermodynamically more stable tetragonal β-In_2S_3 form, which differs from it only in having the cation vacancies ordered according to a specific pattern. The additional XRD peaks of the β-In_2S_3 form, which appear due to the said ordering and are visible in the corresponding reference diffractogram (ref. code 01-084-1385), are not visible here. The diffractogram is thus in agreement with the reference structure and yields a crystal domain size of ca. 37.2 nm using Scherrer's formula.[10,25] Moreover, the crystal domain size value is in agreement with the TEM observed particle size.

The band gap of the synthesized In_2S_3 was determined from the diffuse reflectance UV-Vis spectrum, subjected to the Kubelka-Munk transformation, by means of a Tauc plot (Figure 2). The measurement yielded a 2.1 eV band gap, as deduced from the linear segment in the region above the gap when $(\alpha h\nu)^2$ was plotted against the photon energy (evidencing a direct gap). This result is in agreement with the value obtained for In_2S_3 powder in earlier works[10,25,26] and close to the 2.0 eV value measured for a well crystallized material.[27] The specific area of the In_2S_3 powder was measured using the Brunauer-Emmett-Teller (BET) method, obtaining a value of 40.6 ± 0.3 m^2/g and a total pore volume of 0.168 cm^3/g. The average pore width was 16.5 nm. The pore area distribution is shown in Figure S2.

The surface charge on the In_2S_3 was studied by deposition of the semiconductor particles on LDG electrodes and measuring the interfacial capacitance versus the solution pH by impedance experiments.[28] The In_2S_3-LDG electrode showed a capacitance maximum at pH 7 (Figure S3), which suggests that surface groups have a pKa value around 7.[28,29] Moreover, the capacitance values decreased more when the pH was changed to acidic values than when changed to basic ones. These results suggest that the semiconductor particles are almost without surface charge at pH 5 or lower, whereas there is a net negative charge at neutral pH.[28] This conclusion was

confirmed by the fact that semiconductor particles aggregation was observed at pH 5 and not at pH 7.

Although the CB energy level of In_2S_3 has been reported,[5] we accomplished the electrochemical characterization of a LDG-In_2S_3 modified electrode to evaluate the redox potential of the semiconductor (Figure S4) even knowing that the electrochemical reversibility is not ideal. The value obtained from the standard redox potential is ≈ - 0.2 vs. RHE under irradiation, indicating that there is a fair overpotential to make possible the electron transfer to Hase.

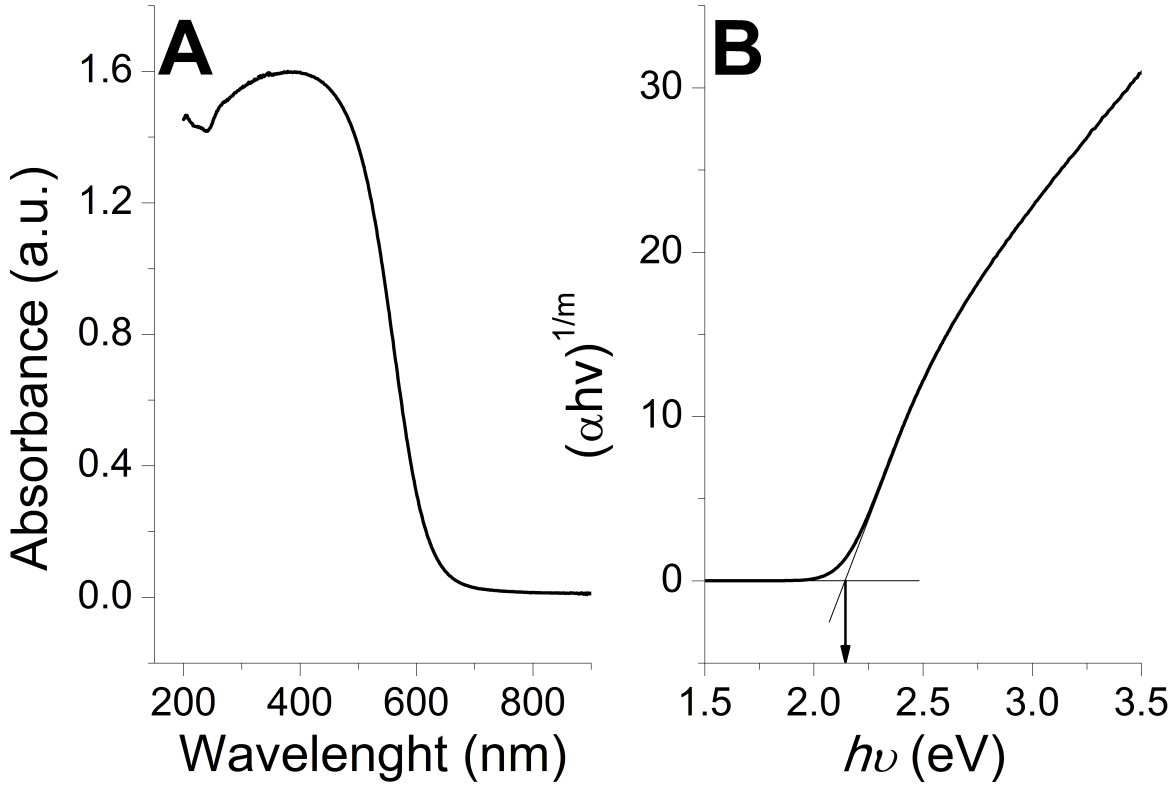

Figure 2. A) UV/Vis absorbance spectrum of In_2S_3. B) Plot of direct band gap of In_2S_3, where α corresponds to absorption coefficient, *h* corresponds to Plank Constant, υ to incident photon

frequency and m correspond to the transition (m=1/2 for direct transition). The arrow marks the band gap value of the semiconductor.

Photoproduction of hydrogen by the hybrid In_2S_3/Hase photocatalyst

Sodium sulfite was chosen as sacrificial compound for the photocatalytic experiments because it has given excellent results with sulfide semiconductors.[6a] Prior to any photoactivity measurement we have measured the effect of the presence of sulfite on the specific activity of the enzyme for H_2 production using reduced methyl viologen at 1 mM concentration as electron donor. The specific activity of *D. vulgaris* [NiFeSe] Hase measured by mass spectrometry in Tris-HCl, pH 7, containing 0.2 M sulfite was 1140 ± 45 μmol $H_2 \times mg^{-1}$ Hase $\times min^{-1}$. In absence of sulfite the specific activity of the enzyme was 3763 ± 221 μmol $H_2 \times mg^{-1} \times min^{-1}$, indicating that sulfite decreased 3-fold the catalytic turnover of the Hase.

The photobiocatalytic production of H_2 was studied using mixtures of Hase and In_2S_3. Such mixtures were prepared by incubating the Hase in presence of In_2S_3 particles dispersed in an aqueous buffer containing 50 mM Tris-HCl 0.2 M sodium sulfite at pH 7. Several incubation periods were tested, after which the catalytic activity of each preparation towards H_2 photosynthesis was measured. Figure 3 shows the H_2 production kinetics for the case in which there was no previous incubation time. The experiment started with the reactor containing only In_2S_3 and sulfite, the electron donor. The solution was irradiated from minute 1 to minute 2 with no production of H_2 during that time frame. Afterwards the Hase sample was injected inside the reaction vessel under dark conditions, allowing 1 min to mix with In_2S_3 under magnetic stirring. When the light was switched on again H_2 production, monitored with the mass spectrometer, was observed almost immediately. Switching off the light source (min 5) interrupted the H_2 production inside the reactor, and after a delay period the H_2 production monitored started to

decrease. When the illumination was restored (min 7) the photobiocatalytic H_2 production rate also was restored. When irradiated the steady state rate of the photocatalytic system was 292 μmol $H_2 \times mg^{-1}$ Hase $\times min^{-1}$, whereas in the absence of light the H_2 production is null. This kinetic experiment shows that a significant amount of In_2S_3-photoexcited electrons that populate the In_2S_3 conductive band (CB) were transferred to the Hase's active site successfully, thus allowing the reduction of two protons to H_2.

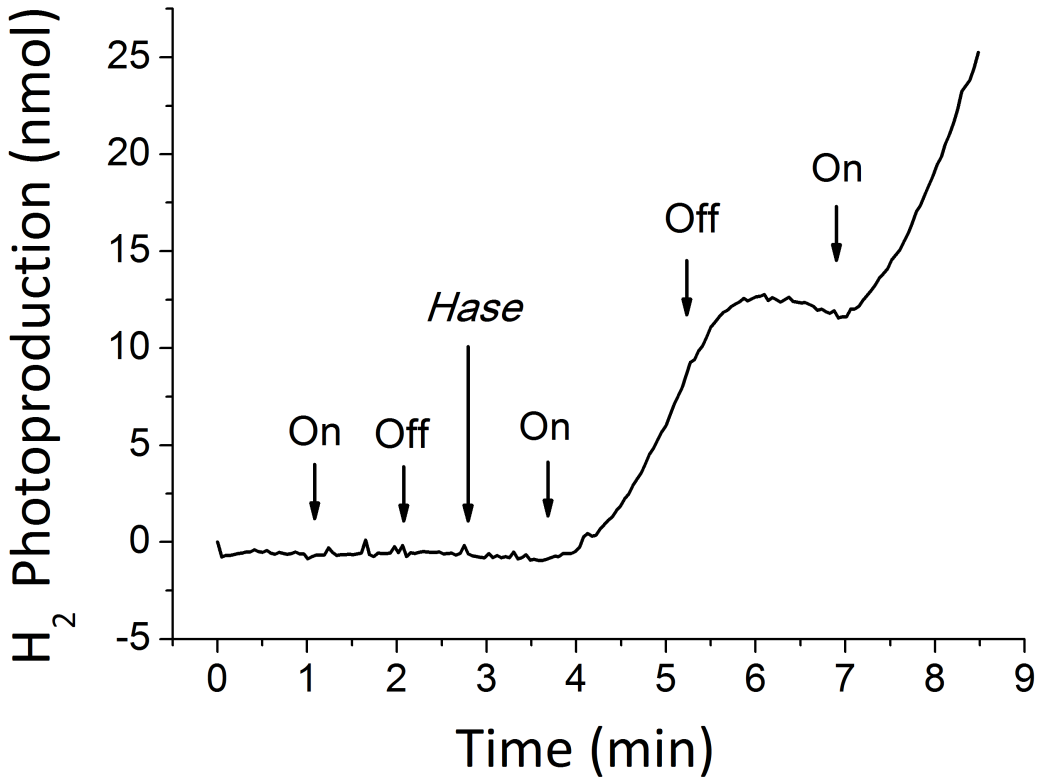

Figure 3. Photocatalytic production of H_2 by *Dv*. [NiFeSe] Hase mixed with In_2S_3 particles monitored by mass spectrometry. The measurements were performed at 37°C in 50mM Tris-HCl, 0.2 M sodium sulfite at pH 7. The arrows mark the times at which the lamp was turned on or off and of Hase injection into the reactor vessel.

Similar kinetic experiments were run for each of the incubation times tested from 0 to 22 h. Figure 4A shows the comparison between an experiment with no previous incubation time (a) and another experiment where the incubation time was 3 h prior to the experiment's run (b). Both samples were exposed to the lamp irradiation during the same period of time, from min 1 to min 3. As it can be observed the longer incubation period yielded a higher H_2 production. The dependence of the specific activity of the hydrogenase for H_2 photobioproduction on the incubation time with the semiconductor is shown in Figure 4B (striped bars). In general terms a longer incubation period yielded a higher photobioproduction of H_2, which did not apply for the overnight incubation period that proved too long (Figure 4B). The highest photobioproduction rate was measured after an incubation time of 6 hours, which was 672 μmol $H_2 \times mg^{-1}$ Hase $\times$ min^{-1}. The H_2 photobioproduction rate for each sample can be compared with the measured H_2 production rate driven by reduced methyl viologen (MV) instead of light, keeping the rest of conditions equal. For these measurements the light was turned off, and 1 mM MV and 0.2 mM sodium dithionite were injected into the reactor. This comparison of catalytic activities allows determining for each sample the efficiency of the photoexcited electron exchange between the In_2S_3 and Hase (Figure 4B, black bars). The initial efficiency of the photocatalytic system with no previous incubation time is 40%, whereas the 6-hour incubation sample yielded 84% H_2-photobioproduction rate efficiency; this means that the irradiated In_2S_3 supplies enough excited electrons to the enzyme. Overnight incubation times were not an improvement. The photobioproduction decreased to 152 μmol $H_2 \times mg^{-1}$ $Hase^{-1} \times min^{-1}$ after 22 hours incubation, whereas the activity with reduced methyl viologen for this sample was 93% of the initial activity of the Hase before incubation with the semiconductor. This result corresponds to 26%

photocatalytic efficiency, indicating that an excess of incubation time scarcely deteriorates the Hase, but it does the In_2S_3 and/or its interface with the Hase.

The photobioactivity towards H_2 production was also tested for either In_2S_3 or Hase as stand-alone catalyst, Figure 4C. Both cases demonstrated to be unable to produce H_2 just when irradiated. In the control experiment with the Hase (Figure 4C, line a) MV was injected at min 4, yielding H_2 production in the absence of light, showing that the Hase was active under these conditions. Regarding the control with In_2S_3, at min 4 of the experiment Hase was added, which turned into H_2 production detection only when the reactor was irradiated. These control experiments show that the photobioproduction of H_2 needs both components, In_2S_3 and Hase, to be successful.

A study of the enzyme ratio attached to the In_2S_3 particles after incubation and their ability to photoproduce H_2 was performed. This study was performed on fresh In_2S_3 samples after different incubation times and consisted on measuring the photoactivity of the Hase/In_2S_3 hybrids to compare them against the activity of Hase remaining in the incubation supernatant. After their incubation time, the samples were let to sediment under natural gravity during 2 hours. The supernatant liquid was then separated from the semiconductor powder sedimented at the bottom. The solid was redispersed with 10 mL of fresh buffer (50 mM Tris-HCl 0.2 M sodium sulfite at pH 7). The H_2 production activity of both fractions was measured by mass spectrometry using 1 mM MV as electron donor. Figure 5 represents the percentage of H_2 production obtained with the supernatant fraction (bars white area) and the semiconductor particles fraction (bars striped area). The black bars also represented in Figure 5 show the percentage of photoactivity in the In_2S_3 particles fraction compared to the Hase activity measured in the same fraction with reduced MV. The total H_2 production activity (sum of the amount obtained with the supernatant and

redispersed fractions) measured with reduced MV for samples incubated 1 h, 3 h, 4 h and 6 h was 687 μmol $H_2 \times mg^{-1}$ Hase $\times min^{-1}$, 1150 μmol $H_2 \times mg^{-1}$ Hase $\times min^{-1}$, 798 μmol $H_2 \times mg^{-1}$ Hase $\times min^{-1}$ and 802 μmol $H_2 \times mg^{-1}$ Hase $\times min^{-1}$ respectively. These results confirmed that the enzyme maintained an average of 75.4% of the initial activity after the incubation and the H_2 photobioproduction assay. The sample incubated during 1h presented 78% of its MV-related enzymatic activity in the In_2S_3-bound fraction, and 49% of it was photocatalytically active. Sample 3h showed an increase of the MV-related enzymatic activity in the In_2S_3-bound fraction up to 92%, whereas only 44% of it was photoactive. Sample 4h retained 85% of the MV-related enzymatic activity within the In_2S_3-bonded fraction, showing an increase up to 61% of the photobiochemicaly produced H_2. Sample 6h showed an 89% MV-related enzymatic activity in the In_2S_3-bonded fraction and the 94% of it was photoactive.

Discussion

The characterization measurements with XRD and TEM of the In_2S_3 revealed that the semiconductor obtained was In_2S_3 in its cubic form, with an average crystal domain size of 37 nm and hexagonal nanocrystal shape. The direct band gap value obtained by UV-VIS spectroscopy at 2.1 eV was the expected for this material,[5] which is thus useful for absorbing light within most of the visible range. SEM images showed that the aggregate particles were spheres mostly about 10 μm diameter; flower like and with high level of porosity where the most common pore size was around 16.5 nm diameter. The diameter of the *Dv* NiFeSe Hase molecules is around 5 nm,[30] which favors the insertion of the enzyme into the semiconductor pores during the incubation process. The impedance spectroscopy results indicated that at pH 7 the semiconductor surface had a negative charge, thus preventing massive aggregation of particles. For this reason, and because the *Dv* NiFeSe Hase has an optimal H_2-production activity

using reduced MV as electron donor at the pH range 6-7,[23] the incubation of enzyme and semiconductor particles was done at pH 7. Our results show that the Hase has great affinity for the semiconductor, as after 1 h incubation most of the active enzyme was attached to the semiconductor particle fraction and not in the solution one. Therefore, we are indeed forming an In_2S_3/Hase hybrid. Such high affinity for the attachment with a semiconductor has also been reported for the NiFeSe Hase from *Desulfomicrobium baculatum* with TiO_2 particles.[31]

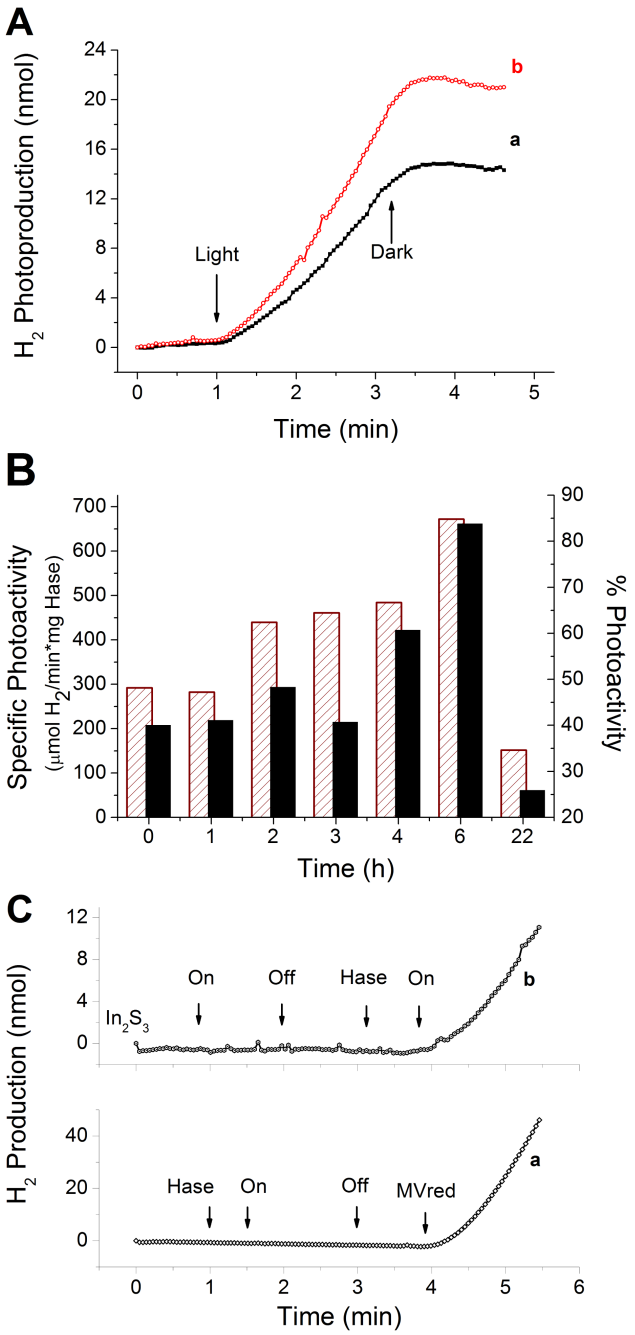

Figure 4. Photocatalytic production of H_2 by *Dv*. [NiFeSe] Hase in combination with In_2S_3 particles monitored by mass spectrometry. Measurements were performed at 37°C in 50 mM Tris-HCl 0.2 M sodium sulfite at pH 7. (A) The lines represent H_2 evolution with no previous incubation of the enzyme with the In_2S_3 (a) or after 3 hours of incubation of Hase with In_2S_3 at 4°C in a roller mixer (b). (B) Striped column bars represent the specific activity of H_2

photoproduction by Hase after different incubation times. Black column bars represent the % of photoactivity of Hase compared to the specific activity of the sample measured with reduced MV as electron donor. (C) Negative controls of photoactivity monitored by mass spectrometry. The lines represent the H_2 evolution under white light illumination with only Hase (a) and only In_2S_3 (b). The arrows mark the time when the light is on or off and the moment when 10μL of 0.166μM Hase or 2 μL of 1 M sodium dithionite is injected into the vessel to reduce the MV.

Irradiation of the mix of Hase and In_2S_3 with visible light clearly led to immediate production of H_2 with a high rate as monitorised *in situ* in aqueous solution by membrane-inlet mass spectrometry. This photocatalytic activity requires both the presence of In_2S_3 and Hase and, as discussed above, both components are attached. Note, however, that mere retention of Hase by In_2S_3 is not enough: while the proportion of Hase retained after only 1 h of incubation is similar to that retained after 6 h (see Fig. 5), more prolonged incubation leads to higher photoactivity. These results suggest that binding the enzyme to the solid to achieve the most active state is a slower process. In any case, it is clear that In_2S_3 is able to excite electrons from its valence band with visible radiation, to use the sulfite in solution as hole scavenger and to transfer the excited electrons at the CB to the efficiently attached Hase, which catalyzes the reduction of 2 protons to H_2. This confirms that the CB has a high enough energy level for thermodynamically favoring the donation of electrons to the Hase, which has a redox potential of approximately -0.4 V vs NHE to drive its catalytic activity.[32] Indeed, the flat-band potentials measured for In_2S_3 films on fluorine-doped tin oxide are between -0.7 and -0.9 V.[33] Efficient photocatalysis with redox metalloenzymes not only requires favorable thermodynamics, it also requires fast kinetics of electron transfer from the semiconductor surface to the exposed redox site of the enzyme (the distal 4Fe4S cluster in the case of hydrogenases).[4]

Our experimental setup is very appropriate for evaluating this step of the photocatalytic process, as we measure the kinetics of product formation directly in the aqueous solution in real time. Furthermore, it allows comparing directly in the same measurement the rate of the photocatalytic process with the hydrogenase specific activity using the standard electron donor for its H_2-production assays: reduced MV.[33] In order to be sure that the kinetics of the overall photocatalytic process were not limited by the photochemical properties of the semiconductor we have done the measurements with a great excess of In_2S_3 over the amount of attached Hase. Thus, we have expressed the H_2-photobioproduction activity per mg of Hase added rather than per mg of the photocatalytic In_2S_3/Hase hybrid. This allows direct comparison with the specific activity of the Hase by the standard procedure and optimization of the In2S3/Hase interface. Our results show that the best photocatalytic results were obtained after 6 hours of incubation of Hase with the In2S3 under mild stirring. Under those conditions, 84% of photocatalytic efficiency is reached when comparing with the total Hase specific activity in solution and on the semiconductor surface, whereas it increases up to 94% when considering only attached Hase. Therefore, we have almost obtained an optimal In2S3/Hase interface in which the photocatalytic process is not rate-limited by electron transfer between semiconductor and enzyme.

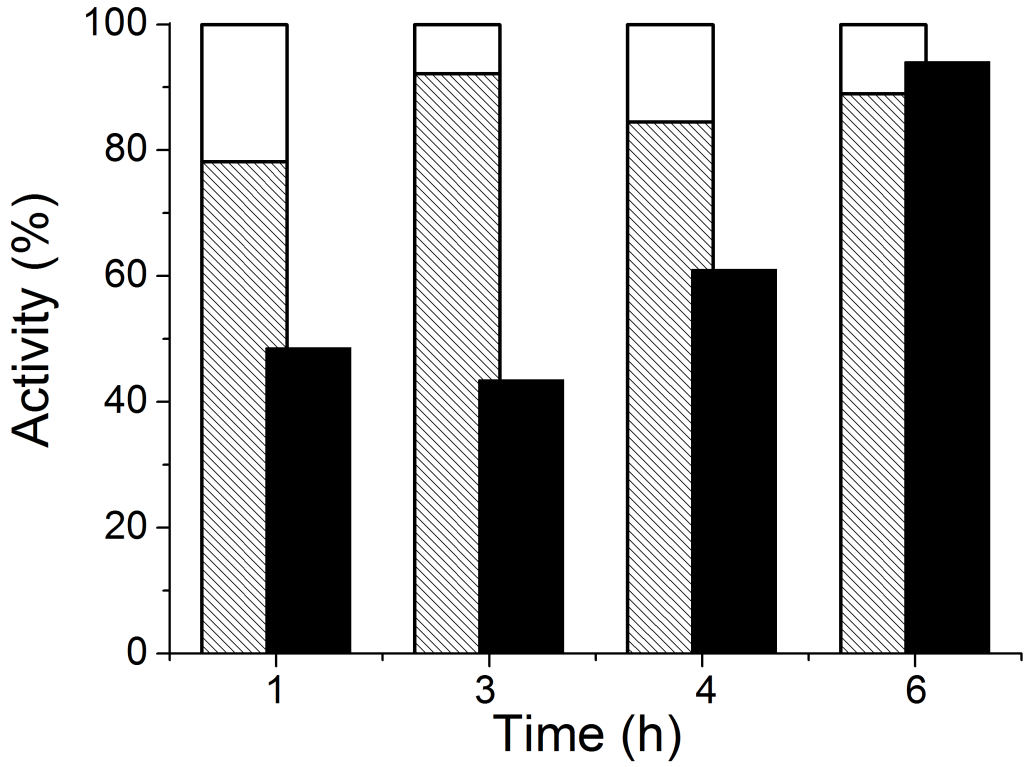

Figure 5. Percentage of *Dv*. [NiFeSe] Hase activity retained by In_2S_3 particles after incubation periods of 1, 3, 4 and 6 hours. The white and striped bar areas represent the % of Hase activity (measured with reduced MV) in the supernatant and In_2S_3 particles fractions respectively. Black bars represent the % of H_2 photobiocatalytic production in the In_2S_3 particles fraction compared to the Hase activity with reduced MV. Measurements were done at 37°C in 50 mM Tris-HCl 0.2 M sodium sulfite at pH 7.

Fast interfacial kinetics of electron exchange of NiFe Hases (including the one used in this work) with electrodes has been obtained by oriented immobilization of the enzyme modulated by electrostatic interactions between charged groups on the electrode surface and the net dipolar moment of the enzyme surface. In this way the distal 4Fe4S cluster of the Hase is facing the electrode surface.[34] A similar strategy was applied by Brown et al. for oriented attachment of an

FeFe hydrogenase to CdS nanorods, in a which very fast Hase turnovers of 380-900 s^{-1} were measured for H_2-photobioproduction.[15] However, in our case the net negative charge of the In_2S_3 surface should not favor adequate orientation of the immobilized NiFeSe Hase for fast electron transfer because the distal 4Fe4S cluster is surrounded by negative charges at neutral pH. Nevertheless, fast interfacial kinetics of electron transfer has also been obtained by adsorption of Hases on rough graphite electrode surfaces with pore diameters slightly larger than the size of the enzyme molecule.[35] In that case, there is a high chance that an enzyme molecule immobilized inside a pore will have its distal 4Fe4S cluster at a distance of the electrode surface adequate for fast direct electron transfer, independently of its orientation.[35] In our case, the highly porous surface of In_2S_3 may favor the inclusion of the enzyme into the cavities of the solid, allowing an efficient contact. The pore analysis of the In_2S_3 indicates an average diameter of 16.5 nm, which is big enough to host the enzyme. Enzymes hosted in such porous cavities are surrounded by the semiconductor surface, increasing the probability that an electron excited in the In_2S_3 migrates to the distal cluster instead of recombining with a hole. The increase in the photobioproduction upon longer incubation times up to 6 h is coherent with slow connection kinetics as explained above. After 1h incubation time almost 80% of the active Hase was bound to the In_2S_3, whereas 20% shows activity in the supernatant fraction; however its photobioproduction rate just reached the 49% of the overall activity. This result indicates a poorly efficient electron transfer from the CB to the Hase active site; the Hase is interacting with the In_2S_3 but the In_2S_3/Hase electron transfer is still rate-limiting. After a 6 h incubation period at 4°C in a roller mixer, the Hase bound to the In_2S_3 reached 89% of the overall activity, which is a small improvement from 1h, but the H_2 photobioproduction rate increased up to 94% efficiency of the bound Hase. The increase in the photobiocatalytic efficiency may be explained by the slow insertion of the Hase

molecules into suitable pores, favoring the contact between the Hase and the surrounding semiconductor and decreasing the importance of Hase orientation for fast electron transfer upon irradiation of the In_2S_3–Hase catalytic tandem. In this way, the highest turnover frequency of the NiFeSe Hase (TOF_{Hase}) we have measured in our system for H_2-photobioproduction was 986 s^{-1}, a value that equals the highest one measured by Brown et al. using CdS nanorods and a FeFe Hase as photocatalyst hybrid.[15]

Conclusions

The present work shows for the first time the H_2 production from water photobiocatalyzed by an In_2S_3-Hydrogenase hybrid catalyst, and powered by visible light. In_2S_3 has been demonstrated as a suitable host for the hydrogenase, managing to transfer the excited electrons into the active site of the enzyme. The optimum experimental conditions comprise an incubation period of 6 hours; this leads to 89% of the hydrogenase being optimally attached to the semiconductor. The photobioproduction of H_2 by this optimal sample was 94% of the total activity measured for the hydrogenase by classical means, proving the importance of an appropriate interfacing between the semiconductor particles and the enzymatic co-catalyst to favor the electron transfer from the In_2S_3 conduction band to the active site of the *D. vulgaris* [NiFeSe] hydrogenase. The result of the present work is of particular interest since it opens the possibility that the whole visible light range, even including a small part of the IR range, may be used for H_2 photo-generation if V-substituted In_2S_3, which has evidenced capability for coupling two low energy excitations like in the Z-scheme of natural photosynthesis,[26] is used as light absorber. Future work founded on the present results will include the study of long-term H_2 photobioproduction and accumulation in gas phase.

ASSOCIATED CONTENT

Supporting Information. Visual details of the In_2S_3 synthesis, pore area analysis and electrochemical characterization are included as supporting information.

AUTHOR INFORMATION

Corresponding Author

* Dr. Marcos Pita: marcospita@icp.csic.es, Dr. Antonio L. De Lacey: alopez@icp.csic.es

Author Contributions

The manuscript was written through contributions of all authors. All authors have given approval to the final version of the manuscript.

Funding Sources

This work was funded by the Spanish MINECO (projects CTQ2015-71290-R and ENE2013-46624-C4-1-R) and by Fundação para a Ciência e Tecnologia (Portugal) (Grants UID/Multi/04551/2013 and PTDC/BBB-BEP/2885/2014 and PhD fellowship SFRH/BPD/xxx/201x). C. T. thanks the Spanish MINECO for her BES-2013-064099 contract.

Notes

The authors declare no financial competing interest.

REFERENCES

(1) a) Navarro, R. M.; Peña, M. A.; Fierro, J. L. G. *Chem. Rev.* 2007, *107*, 3952-3991. b) Grigoriev, S.; Porembsky, V.; Fateev, V. *Int. J. Hydrogen Energy,* **2006**, *31*, 171-175.

(2) Tachibana, Y.; Vayssieres, L.; Durrant, J. *Nat Photonics* **2012**, *6*, 511-518.

(3) a) Xu, Y.; Xu, R. *Appl. Surf. Sci.,* **2015**, *351*, 779-793. b) Cheng, H.; Lv, X. J.; Cao, S.; Zhao, Z. Y.; Chen, Y.; Fu, W. F. *Scientific Reports,* **2016**, *6*, 19846.

(4) Bachmeier, A.; Armstrong, F. *Current Op. Chem. Biol.* **2015**, *25*, 141-151.

(5) (a) Becker, R. S.; Zheng, T.; Elton, J.; Saeki, M. *Sol. Energ. Mat.* 1986*, 13*(2), 97-107. (b) Xu, Y.; Schoonen, M. A. A. *Am. Mineralogist,* **2000**, *85*, 543-556.

(6) a) Zhang, K.; Guo, L. *Catal. Sci. Technol.* 2013, *3*, 1672-1690. b) Iwashina, K.; Iwase, A.; Ng, Y. H.; Amal, R.; Kudo, A. *J. Am. Chem. Soc.* **2015**, *137*, 604-607.

(7) (a) Bakke, J. R.; Pickrahn, K. L.; Brennan, T. P.; Bent, S. F. *Nanoscale* **2011**, *3*, 3482-3508. (b) Mughal, M. A.; Engelken, R.; Sharma, R. *Solar Energy* 2015, *120*, 131-146. (c) Hariskos, D.; Spiering, S.; Powalla, M. *Thin Solid Films* **2005**, *480–481*, 99 – 109 (d) Spiering, S.; Hariskos, D.; Powalla, M.; Naghavi, N.; Lincot, D. *Thin Solid Films* **2003**, *431 – 432*, 359–363.

(8) Jiang,F.; Gunawan, Harada, T.; Kuang, Y.; Minegishi, T.; Domen, K.; Ikeda, S. *J. Am. Chem. Soc.* **2015**, *137*, 13691-13697.

(9) Cingarapu, S.; Ikenberry, M. A.; Hamal, D. B.; Sorensen, C. M.; Hohn, K.; Klabunde, K. J. *Langmuir* **2012**, *28*, 3569–3575.

(10) Lucena, R.; Aguilera, I.; Palacios, P.; Wahnón, P.; Conesa, J. C. *Chem. Mater.* **2008**, *20*, 5125-5127.

(11) De Lacey, A. L. ; Fernandez, V. M. ; Rousset, M.; Cammack, R. *Chem. Rev.* **2007**, *107*, 4304-4330.

(12) Fontecilla-Camps, J. C.; Volbeda, A.; Cavazza, C.; Nicolet, Y. *Chem. Rev.,* **2007**, *107*, 4273-4303.

(13) Cracknell, J. A.; Vincent, K. A.; Armstrong, F. A. *Chem. Rev.,* 2008, **108**, 2439-2461.

(14) Caputo, C. A.; Wang, L.; Beranek, R.; Reisner, E. *Chem. Sci.* **2015**, *6*, 5690-5694.

(15) Brown, K. A.; Wilker, M. B.; Boehm, M.; Dukovic, G.; King, P. W. *J. Am. Chem. Soc.* **2012**, *134*, 5627-5636.

(16) a) Brown, K. A.; Dayal, S.; Ai, X.; Rumbles, G.; King, P. W. *J. Am. Chem. Soc.* **2010**, *132*, 9672-9680. b) Greene, B. L.; Joseph, C. A.; Maroney, M. J.; Dyer, R. B. *J. Am. Chem. Soc.,* **2012**, *134*, 11108-11111.

(17) Caputo, C. A.; Gross, M. A.; Lau, V. W.; Cavazza, C.; Lotsch, B. V.; Reisner, E. *Angew. Chem. Int. Ed.* **2014**, *53*, 11538-11542.

(18) a) Goldet, G.; Wait, A. F.; Cracknell, J. A.; Vincent, K. A.; Ludwig, M.; Lenz, O.; Friedrich, B.; Armstrong, F. A. *J. Am. Chem. Soc.,* **2008,** *130*, 11106-11113. b) Sakai, T.; Mersch, D.; Reisner, E. *Angew. Chem. Int. Ed.* **2013**, *52*, 12313-12316.

(19) Baltazar, C. S. A.; Marques, M. C.; Soares, C. M.; De Lacey, A. L.; Pereira I. A. C.; Matias, P. M. *Eur. J. Inorg. Chem.* **2011**, 7,948-962.

(20) Utterback, J. K.; Wilker, M. B.; Brown, K. A.; King, P. W.; Eaves, J. D.; Dukovic, G. *Phys. Chem. Chem. Phys.* **2015**, *17*, 5538-5542.

(21) Wilker, M. B.; Shinopoulos, K. E.; Brown, K. A.; Mulder, D. W.; King, P. W.; Dukovic, G. *J. Am. Chem. Soc.* **2014**, *136*, 4316-4324.

(22) a) Jouanneau, Y.; Kelley, B. C.; Berlier, Y.; Lespinat, P. A.; Vignais, P. M. *J. Bacteriol*., **1980**, *143*, 628-636.

(23) Valente, F. M. A.; Oliveira, A. S. F.; Gnadt, N.; Pacheco, I.; Coelho, A. V.; Xavier, A. V.; Teixeira, M.; Soares, C. M.; Pereira, I. A. C. *J. Biol. Inorg. Chem.,* **2005**, *10*, 667-682.

(24) a) Vignais, P. M.; Cournac, L.; Hatchikian, E. C.; Elsen, S.; Serebryakova, L.; Zorin N.; Dimon, B.. *Int J. Hydrogen Energy*, **2002**, *27*, 1441-1448. b) Gutiérrez-Sanz, O.; Marques, M. C.; Baltazar, C. A.; Fernández, V. M.; Soares, C.M.; Pereira I. A. C.; De Lacey, A. L. *J. Biol. Inorg. Chem*. **2013**, *18*, 419-427.

(25) Lucena, R.; Conesa, J. C.; Aguilera, I.; Palacios, P.; Wahnón, P. *J. Mater. Chem. A*, **2014**, *2*, 8236-8245.

(26) Lucena, R.; Fresno, F.; Conesa, J. C. *Catal. Commun.,* **2012**, *20*, 1-5.

(27) Kambas, K.; Anagnostopoulos, A.; Ves, S.; Ploss, B.; Spyridelis, J. *Physica Status Solidi*(b), **1985**, *127*, 201-208.

(28) Bryant, M. A.; Crooks, R. M. *Langmuir,* **1993**, *9*, 385-387.

(29) Smith, C. P.; White, H. S. *Langmuir,* **1993**, *9*, 1-3.

(30) Marques, M. C.; Coelho, R.; De Lacey, A. L.; Pereira, I. A. C.; Matias, P. M. *J. Mol. Biol.,* **2010**, *396*, 893-907.

(31) Reisner, E.; Powell, D. J.; Cavazza, C.; Fontecilla-Camps, J. C.; Armstrong, F. A. *J. Am. Chem. Soc.,* **2009**, *131*, 18457-18466.

(32) De Lacey, A. L.; Gutiérrez-Sánchez, C.; Fernández, V. M.; Pacheco, I.; Pereira, I. A. C. *J. Biol. Inorg. Chem.*, **2008**, *13*, 1315-1320.

(33) Cammack, R.; Frey, M.; Robson, R. *Hydrogen as a Fuel: Learning from Nature*. Taylor & Francis, **2001**, London, New York.

(34) a) Rüdiger, O.; Abad, J. M.; Hatchikian, E. C.; Fernandez, V. M.; De Lacey, A. L. *J. Am. Chem. Soc.*, **2005**, *127*, 16008-16009. b) Rüdiger, O.; Gutiérrez-Sánchez, C. ; Olea, D. ; Pereira, I. A. C.; Vélez, M. ; Fernández, V. M. ; De Lacey, A. L. *Electroanalysis*, **2010**, *22*, 776-783.

(35) Hexter, S. V.; Esterle, T. F.; Armstrong, F. A. *Phys. Chem. Chem. Phys.* **2014**, *16*, 11822-33.

SYNOPSIS

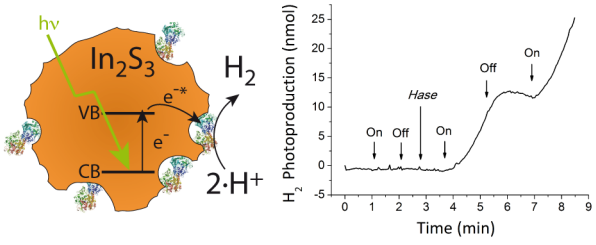

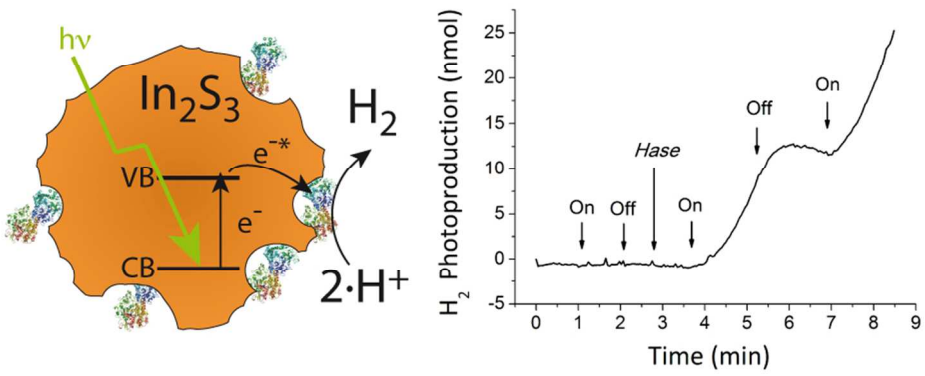

TOC
84x34mm (300 x 300 DPI)